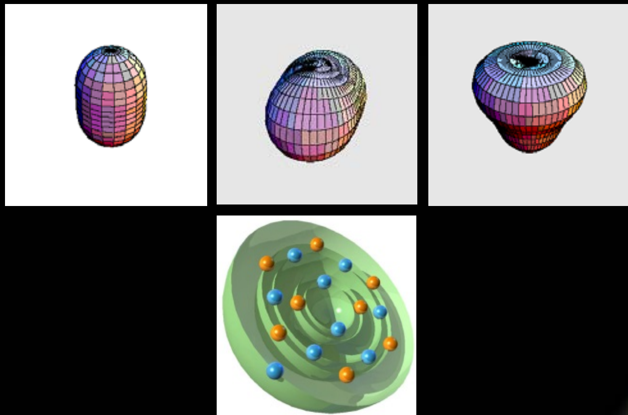

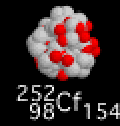

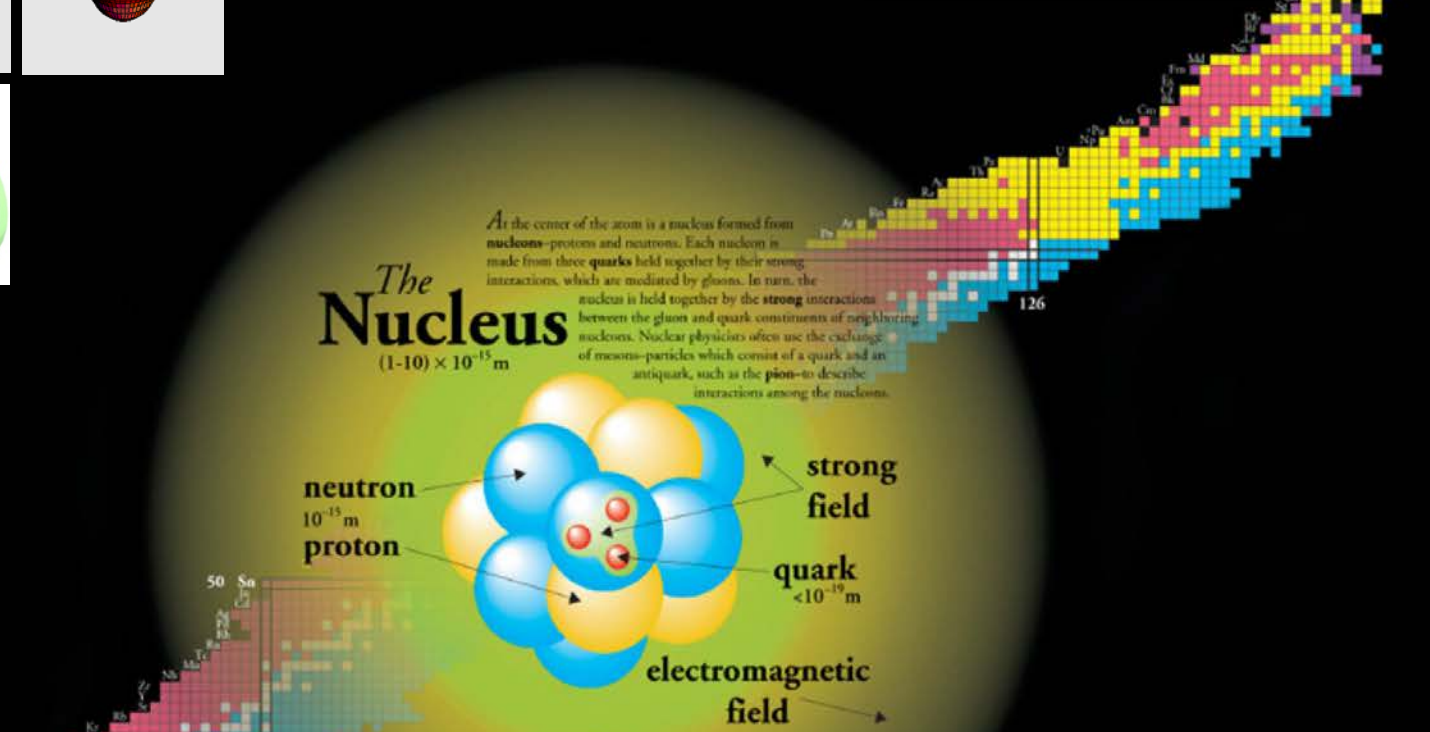

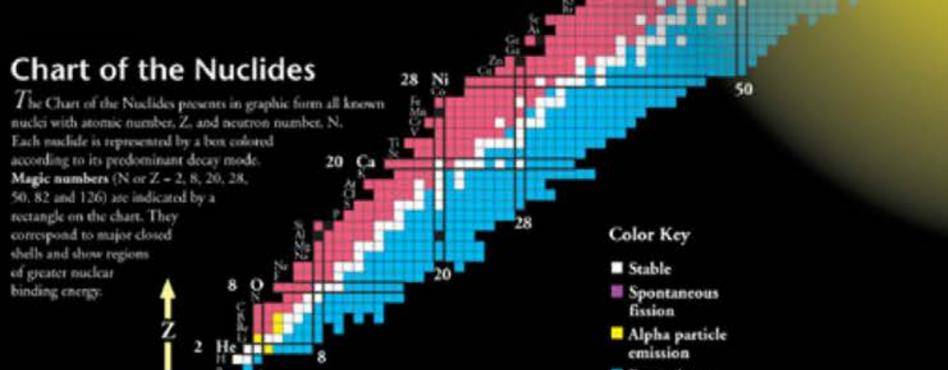

heavy ion
nuclear reactions

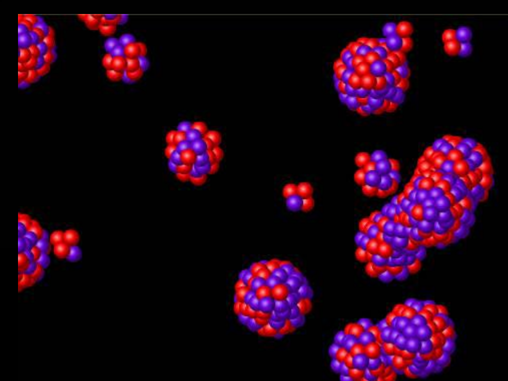

Heavy ion nuclear reactions

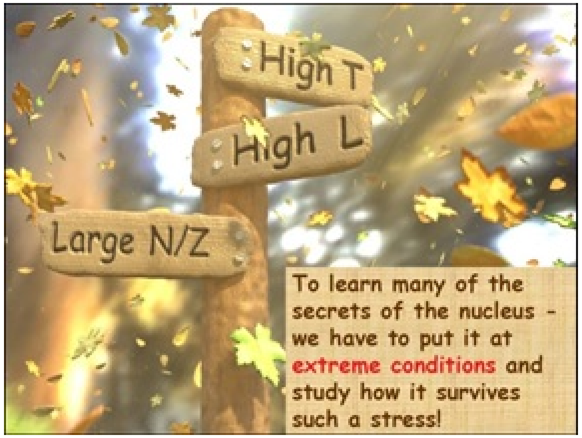

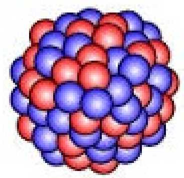

SIS-18

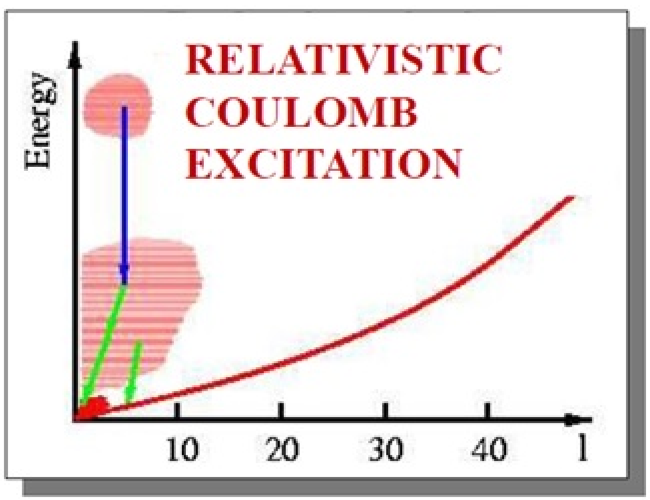

UNILAC

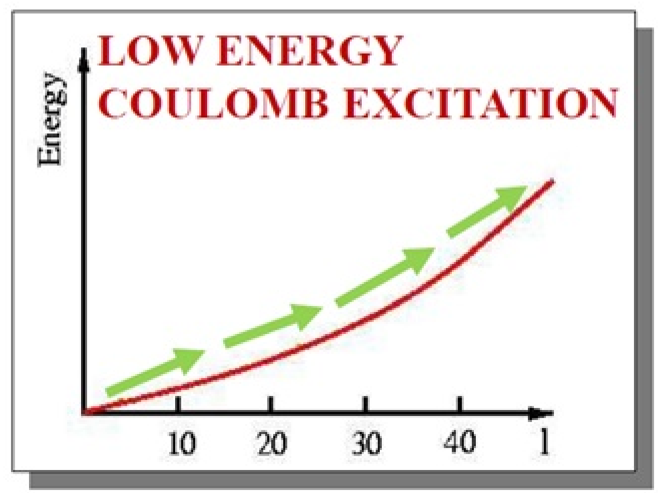

Count rate estimate

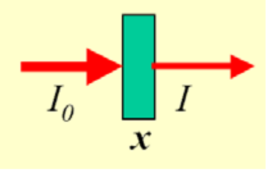

Reaction rate [s^{-1}] = luminosity · cross section [cm^2]
= projectiles [s^{-1}] · target nuclei [cm^{-2}] · cross section [cm^2]

accelerator current: 1 pnA consists of $6 \cdot 10^9$ projectiles [s^{-1}]

target thickness: 1 mg/cm^2 $\quad \dfrac{6 \cdot 10^{23} \cdot 10^{-3} [g/cm^2]}{A_{target}[g]} = target\ nuclei\ [cm^{-2}]$

A_{target}	target nuclei	projectiles	luminosity [s^{-1} cm^{-2}]
200	$3 \cdot 10^{18}$ [cm^{-2}]	$6 \cdot 10^9$ [s^{-1}]	$18 \cdot 10^{27}$ [s^{-1} cm^{-2}]
100	$6 \cdot 10^{18}$ [cm^{-2}]	"	$36 \cdot 10^{27}$ [s^{-1} cm^{-2}]
50	$12 \cdot 10^{18}$ [cm^{-2}]	"	$72 \cdot 10^{27}$ [s^{-1} cm^{-2}]

beam structure: 50 Hz 5 ms

duty factor: 25%

Coulomb excitation: particle identification

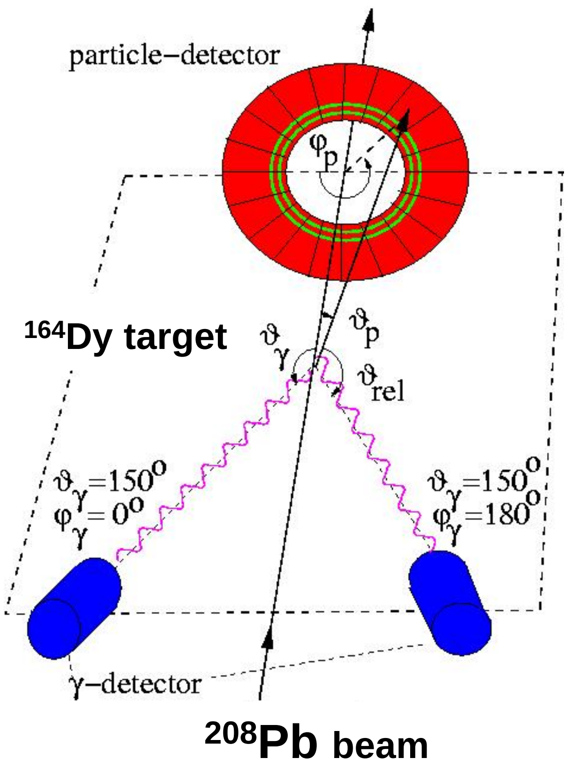

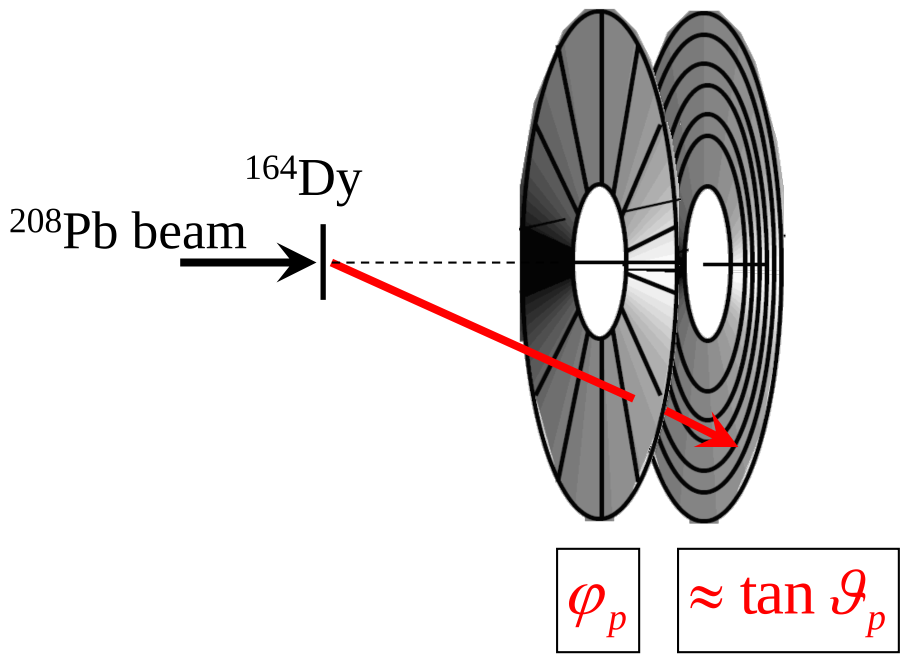

V_0 ~ 500 V
p = 5-10 Torr
gap ~ 3 mm (anode-cathode)

distance target – PPAC: 11 cm

Coulomb excitation: particle identification

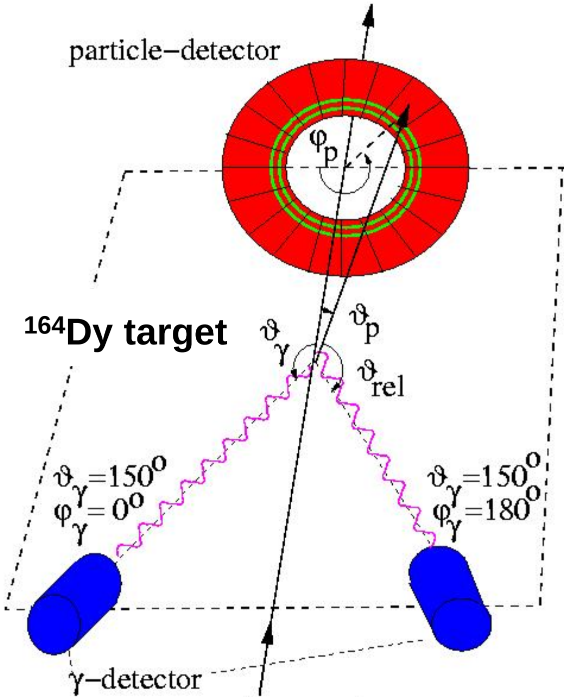

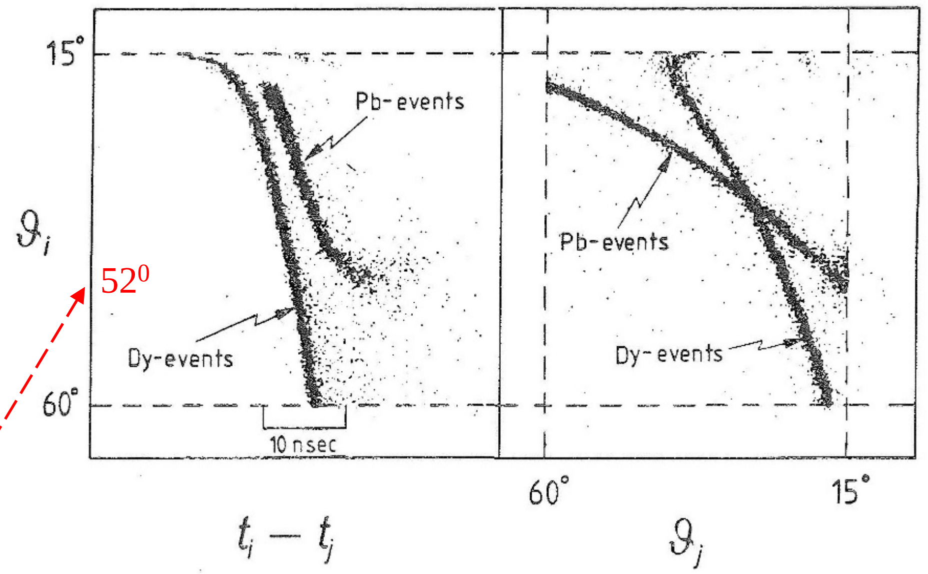

$$max.\, scattering\ angle = arc\ sin \frac{A_2}{A_1}$$

distance target – PPAC: 11 cm

Doppler shift correction

^{208}Pb + ^{164}Dy at 978 MeV

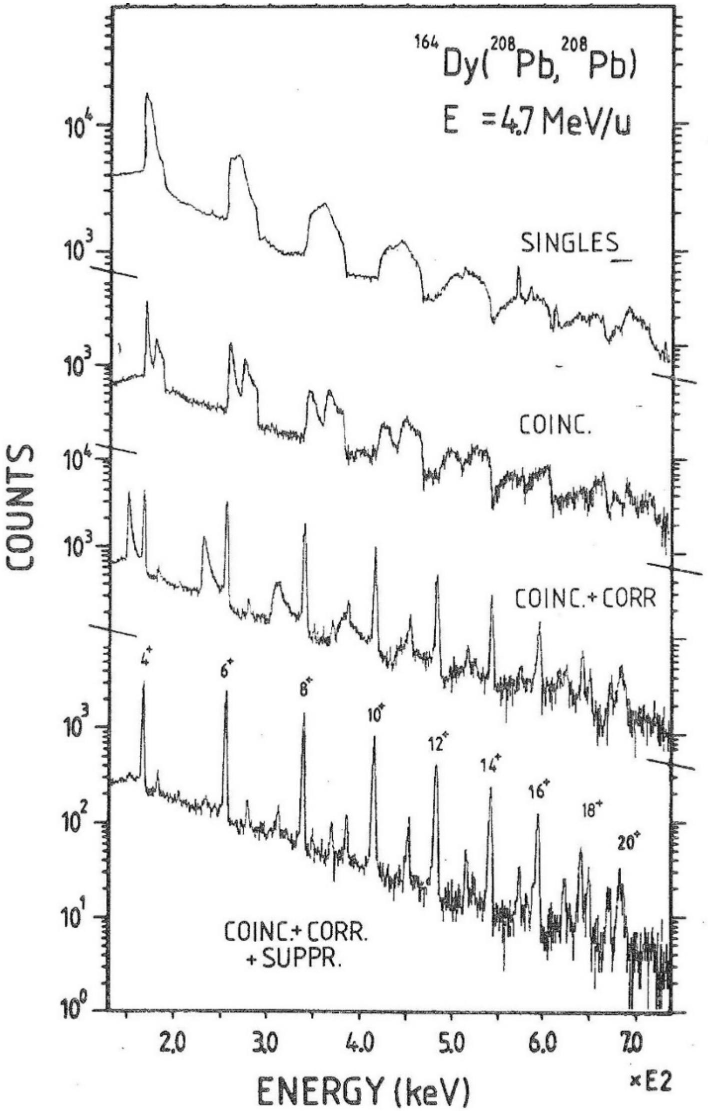

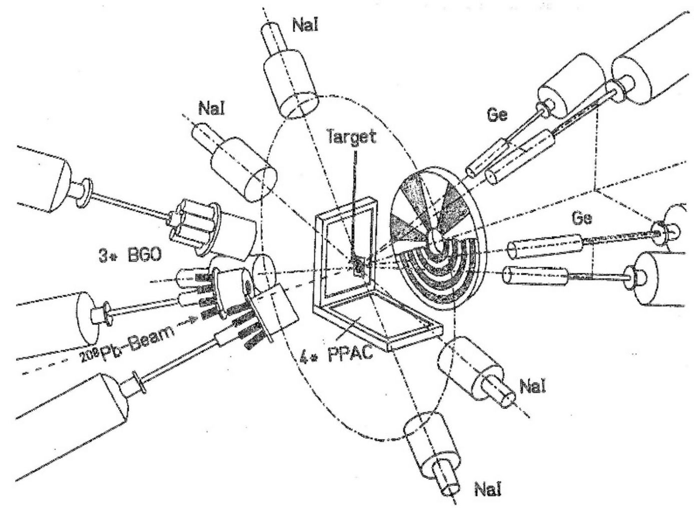

^{164}Dy **target nucleus measured with PPAC** (^{164}Dy **target excitation**)

index 1≡projectile (^{208}Pb) index 2≡target nucleus (^{164}Dy)

$$v_{cm} = 0.04634 \cdot \left(1 + A_2 / A_1\right)^{-1} \sqrt{E_{\ell ab} / A_1}$$ (=0.02746)

$$v_2 = 2 \cdot v_{cm} \cdot \cos\vartheta_2$$

$$\cos\vartheta_{\gamma 2} = \cos\vartheta_\gamma \cdot \cos\vartheta_2 + \sin\vartheta_\gamma \cdot \sin\vartheta_2 \cdot \cos\left(\varphi_\gamma - \varphi_2\right)$$

$$\cos(\varphi_\gamma - \varphi_2) = \cos\varphi_\gamma \cdot \cos\varphi_2 + \sin\varphi_\gamma \cdot \sin\varphi_2$$

$$\boxed{\frac{E_{\gamma 0}}{E_\gamma} = \frac{1 - v_2 \cdot \cos\vartheta_{\gamma 2}}{\sqrt{1 - v_2^2}}}$$

D. Schwalm et al. Nucl.Phys. A192 (1972), 449

The reorientation effect

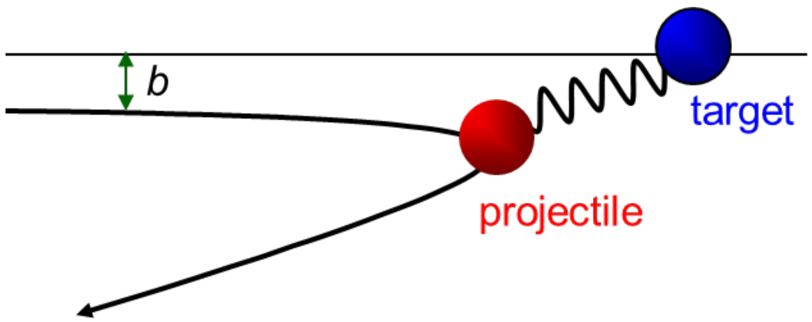

The excitation cross section is a direct measure of the $E\lambda$ matrix elements.

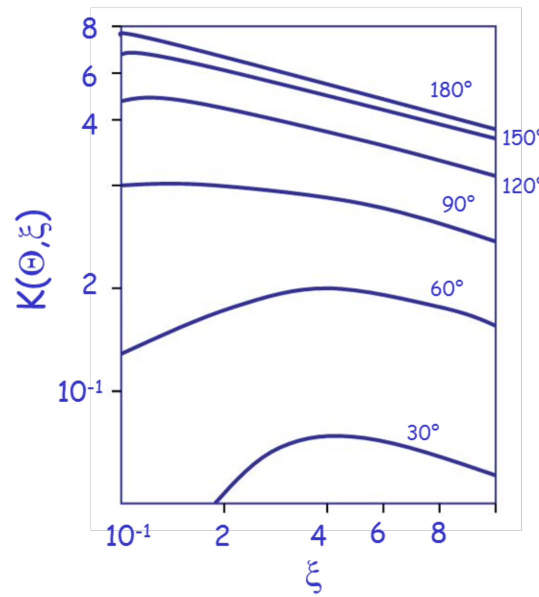

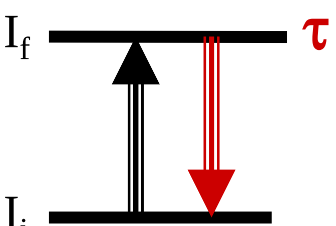

1st order:

$$a^{(1)}_{i\to f} \propto \langle I_f \| \mathbf{M}(E2) \| I_i \rangle$$

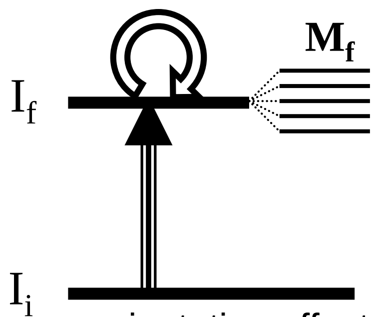

reorientation effect:

$$a^{(2)}_{i\to f} \propto \langle I_f \| \mathbf{M}(E2) \| I_f \rangle \langle I_f \| \mathbf{M}(E2) \| I_i \rangle$$

$$P^{(2)}_{0\to 2}(\theta,\xi) = P^{(1)}_{0\to 2}(\theta,\xi) \cdot \left[1 + \sqrt{\frac{7}{2\pi}\frac{5}{4}} \cdot \frac{A_p}{Z_p} \cdot \frac{\Delta E}{1 + A_p/A_t} \cdot Q_2 \cdot K(\theta,\xi) \right]$$

$$Q(2^+) = -\sqrt{\frac{2\pi}{7}\frac{4}{5}} \cdot \langle 2 \| M(E2) \| 2 \rangle$$

Quadrupole deformation in ^{182,184,186}W

W176 2.5 h 0+ EC	W177 135 m (1/2-) EC	W178 21.6 d 0+ EC	W179 37.05 m (7/2)- * EC	W180 0+ * 0.13	W181 121.2 d 9/2+ EC	W182 0+ 26.3	W183 1.1E+17 y 1/2- * 14.3	W184 3E+17 y 0+ 30.67	W185 75.1 d 3/2- * β-	W186 0+ 28.6	W187 23.72 h 3/2- β-	W188 69.4 d 0+ β-	W189 11.5 m (3/2-) β-	W190 30.0 m 0+ β-
Ta175 10.5 h 7/2+ EC	Ta176 8.09 h (1)- * EC	Ta177 56.56 h 7/2+ EC	Ta178 9.31 m 1+ * EC	Ta179 1.82 y 7/2+ * EC	Ta180 8.152 h 1+ EC,β- 0.012 *	Ta181 7/2+ 99.988	Ta182 114.43 d 3- * β-	Ta183 5.1 d 7/2+ β-	Ta184 8.7 h (5-) β-	Ta185 49.4 m (7/2+) β-	Ta186 10.5 m 2,3 β-	Ta187	Ta188	116
Hf174 2.0E15 y 0+ α 0.162	Hf175 70 d 5/2- EC	Hf176 0+ 5.206	Hf177 7/2- * 18.606	Hf178 0+ * 27.297	Hf179 9/2+ * 13.629	Hf180 0+ * 35.100	Hf181 42.39 d 1/2- β-	Hf182 9E6 y 0+ * β-	Hf183 1.067 h (3/2-) β-	Hf184 4.12 h 0+ β-	Hf185 3.5 m β-	Hf186 0+		

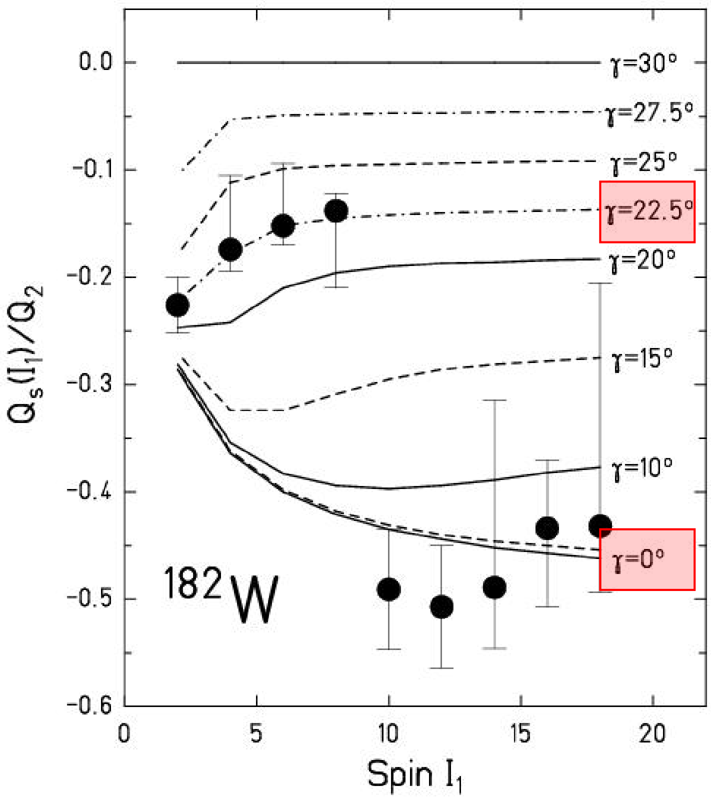

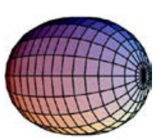

prolate

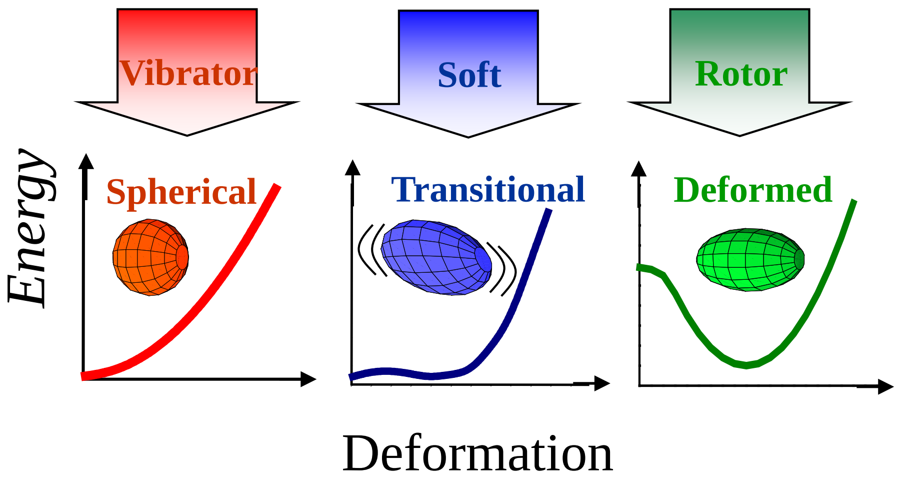

R. Kulessa et al., Phys. Lett. B218 (1989), 421

Alignment of $i_{13/2}$ protons in ^{242,244}Pu

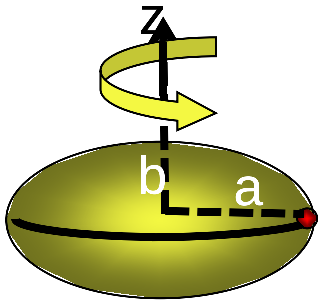

$$E_I = \frac{\hbar^2}{2\mathfrak{I}} I(I+1)$$

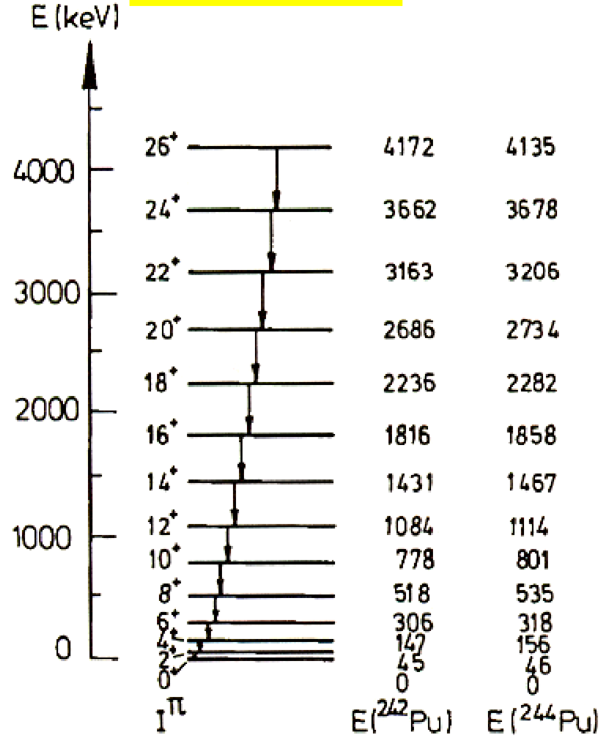

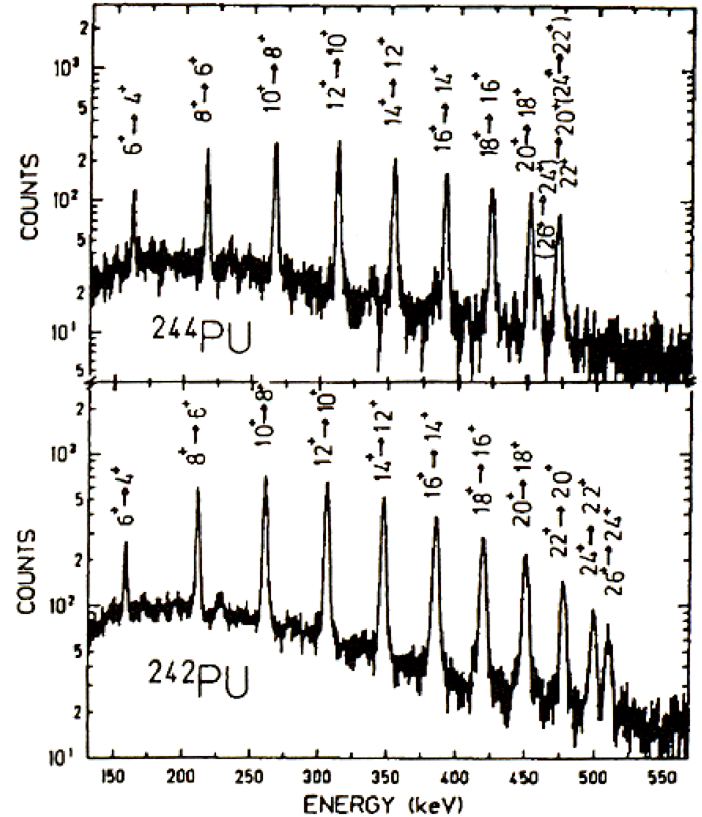

$$E_\gamma = E_I - E_{I-2} = \frac{\hbar^2}{2\mathfrak{I}}(4I-2)$$

$$\mathfrak{I} = \frac{2}{5} A \cdot M \cdot R_0^2 \cdot \beta^2$$

$$B(E2; I \rightarrow I-2) = \frac{15}{32\pi} \frac{I(I+1)}{(2I-1)(2I+1)} \cdot Q_2$$

$$Q_2 = \frac{3ZR_0^2}{\sqrt{5\pi}} \cdot \beta$$

- analysis with GOSIA code

W. Spreng et al., Phys. Rev. Lett. 51 (1983), 1522

Coulomb excitation of ^{114}Sn

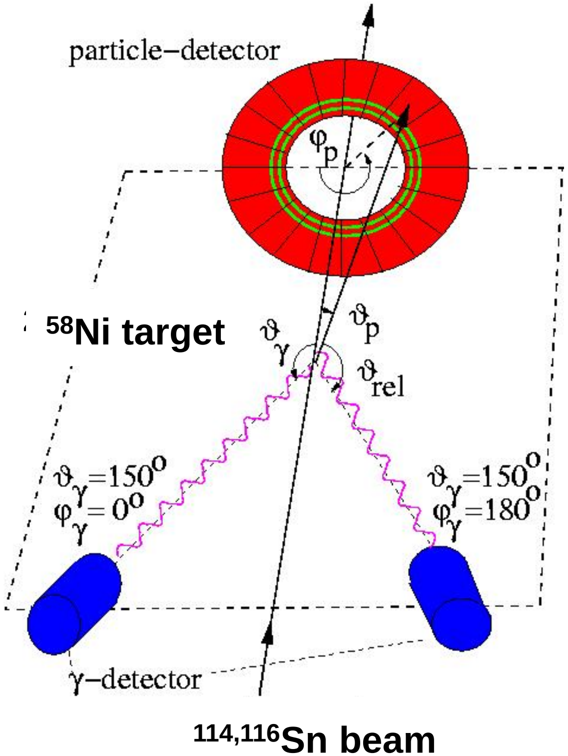

^{114,116}Sn→^{58}Ni at 3.6MeV/u

E_x=1300, 1294 MeV
B(E2)↑=0.25(5), 0.209(5)e^2b^2

γ-efficiency = 0.005
accelerator duty factor=10%

beam intensity = 1pnA
target thickness = 1mg/cm^2

pγ-rate (Sn) = 1/s

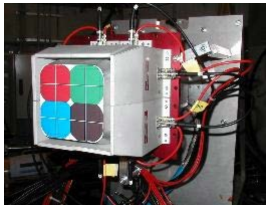

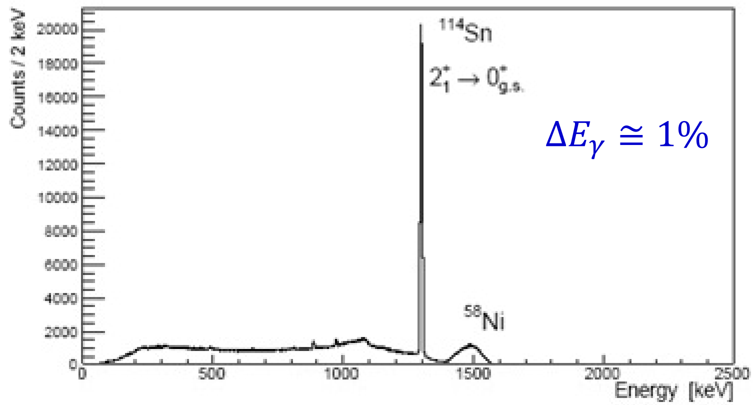

natural abundance of ^{114}Sn: 0.65%

P. Doornenbal, A.Jhingan, R.Kumar, et al., Phys.Rev C 78 (2008) 031303

α-transfer reactions

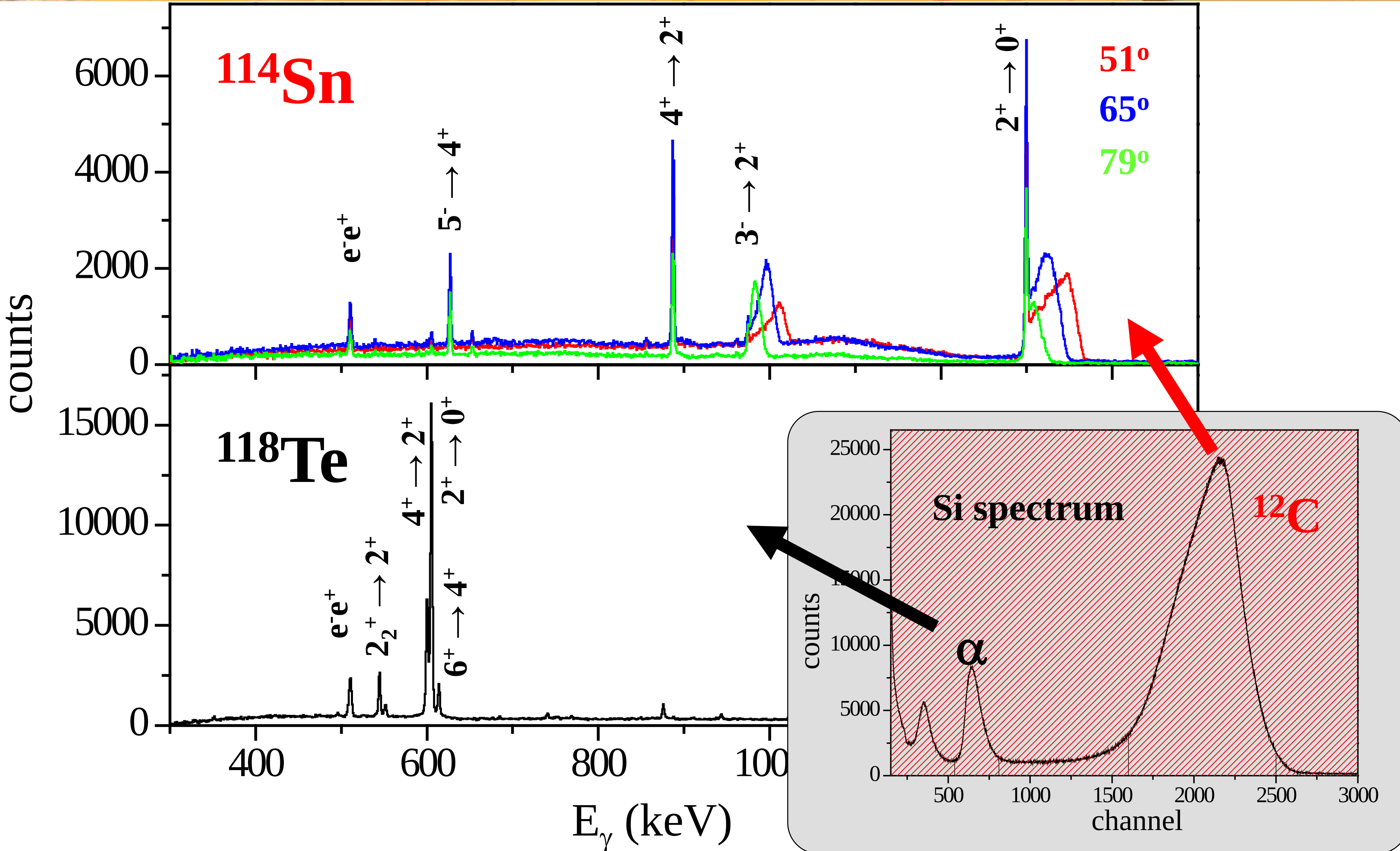

Space inversion invariance: octupole deformed nucleus ^{226}Ra

$|\Psi\rangle = |$ 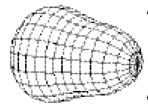 $\rangle$

$P|\Psi\rangle = |$ 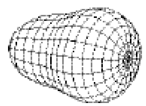 $\rangle$

$$P|\Psi\rangle \neq |\Psi\rangle$$

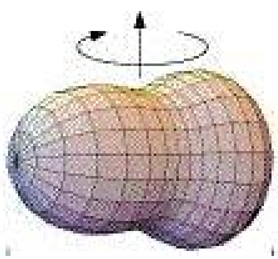

rotation

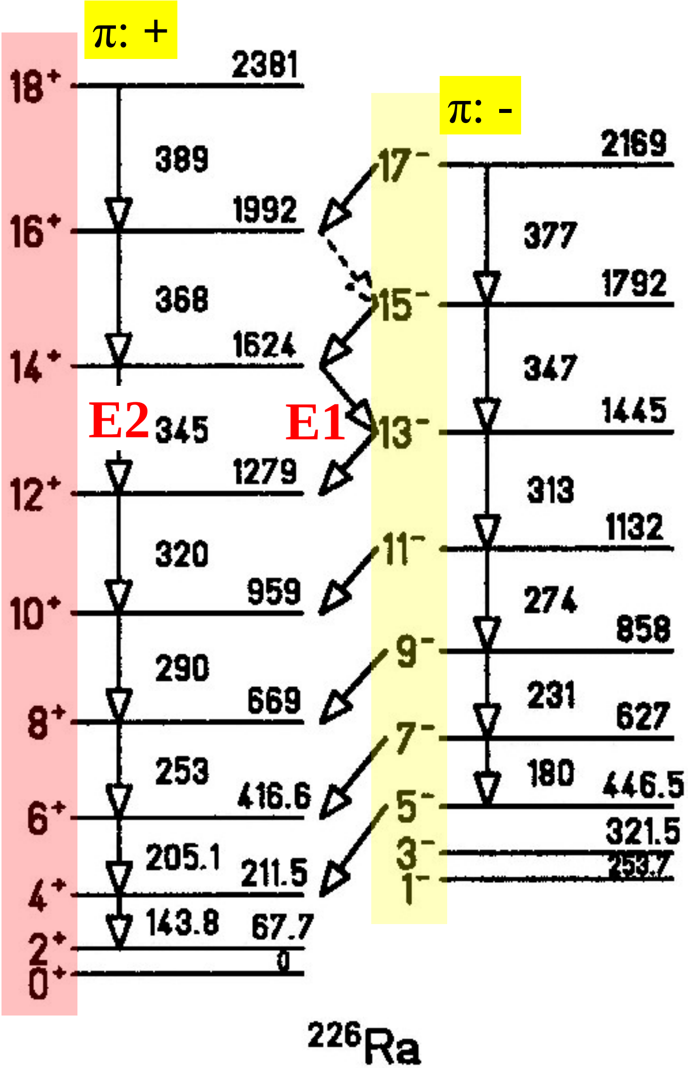

H.J.Wollersheim, C. Fleischmann et al., Nucl. Phys. A556 (1993), 261

Coulomb excitation of ^{226}Ra

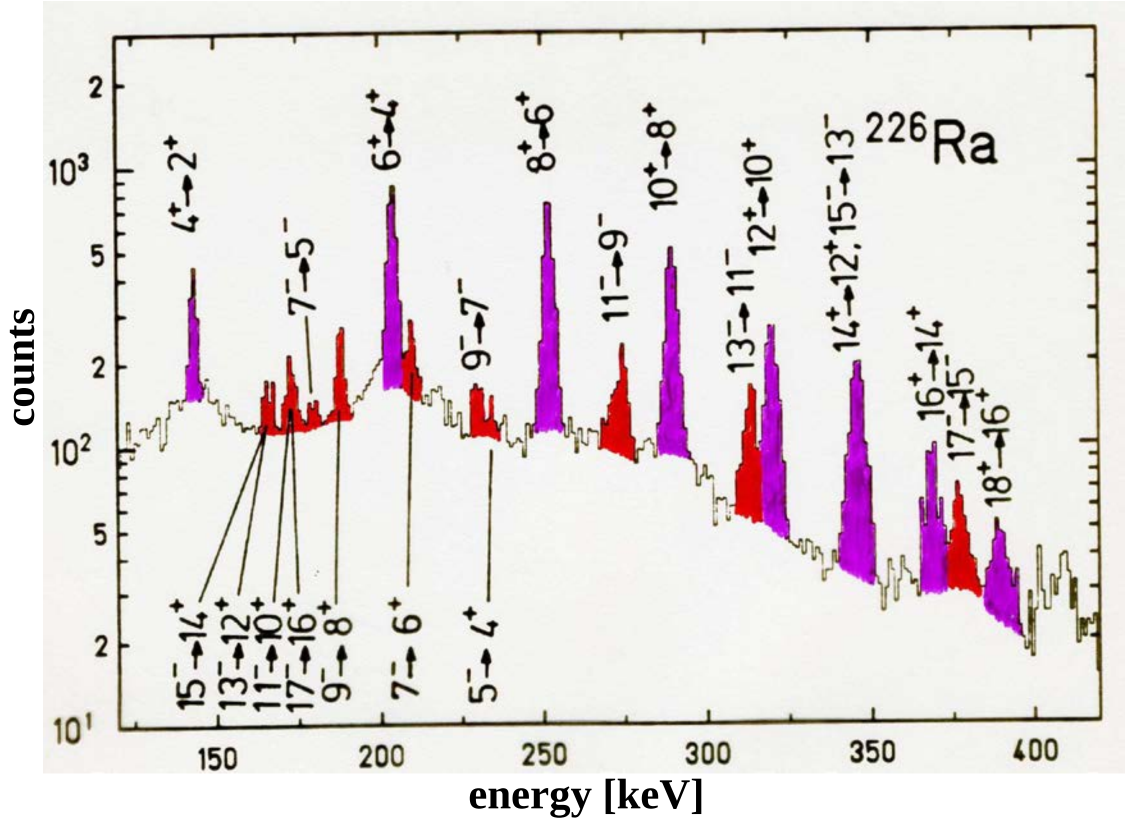

$^{208}Pb \longrightarrow {}^{226}Ra$

$E_{lab} = 4.7$ AMeV

$15^0 \leq \theta_{lab} \leq 45^0$

$0^0 \leq \varphi_{lab} \leq 360^0$

^{226}Ra target broken after 8 hours

Conversion electrons

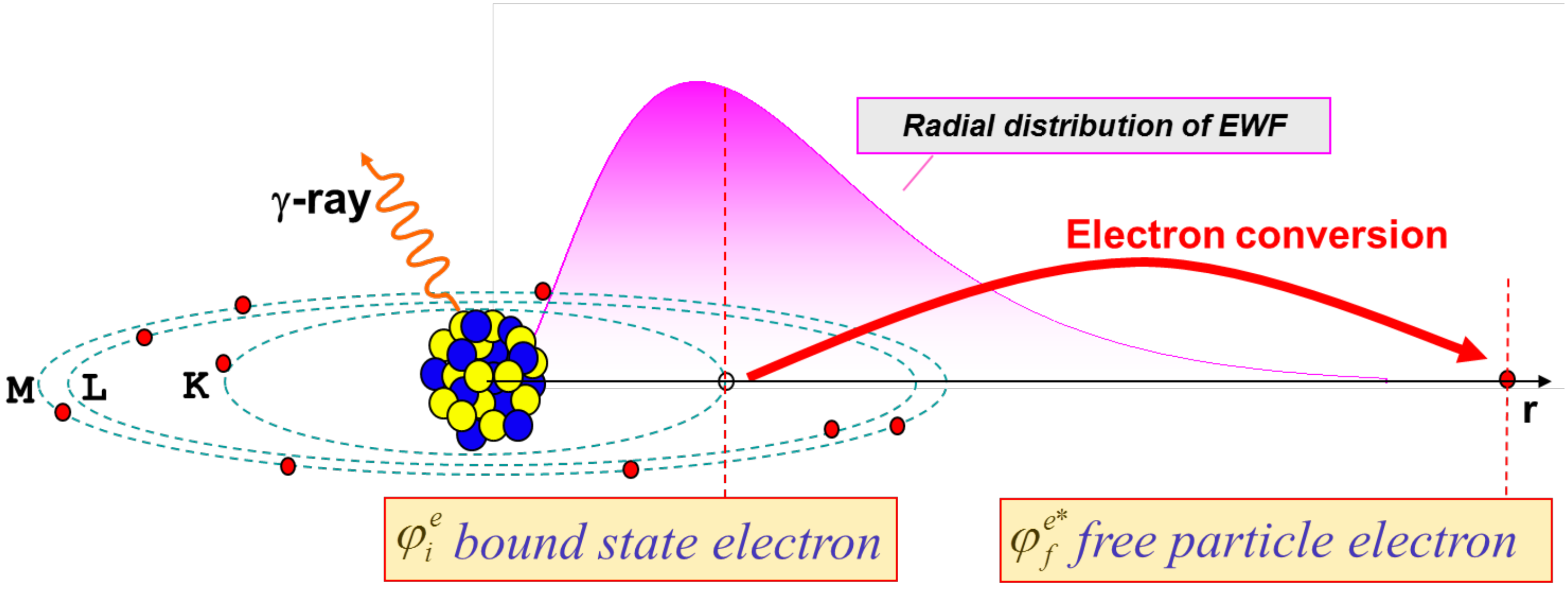

❖ For an electromagnetic transition internal conversion can occur instead of emission of gamma radiation. In this case the transition energy $Q = E_\gamma$ will be transferred to an electron of the atomic shell.

$$\boxed{T_e = E_\gamma - B_e}$$

T_e: kinetic energy of the electron
B_e: binding energy of the electron

internal conversion is important for:
- heavy nuclei ~ Z^3
- high multipolarities Eℓ or Mℓ
- small transition energies

$$\alpha_k(El) \propto Z^3 \left(\frac{L}{L+1}\right)\left(\frac{2m_e c^2}{E}\right)^{L+5/2}$$

Electron spectroscopy with Mini-Orange devices

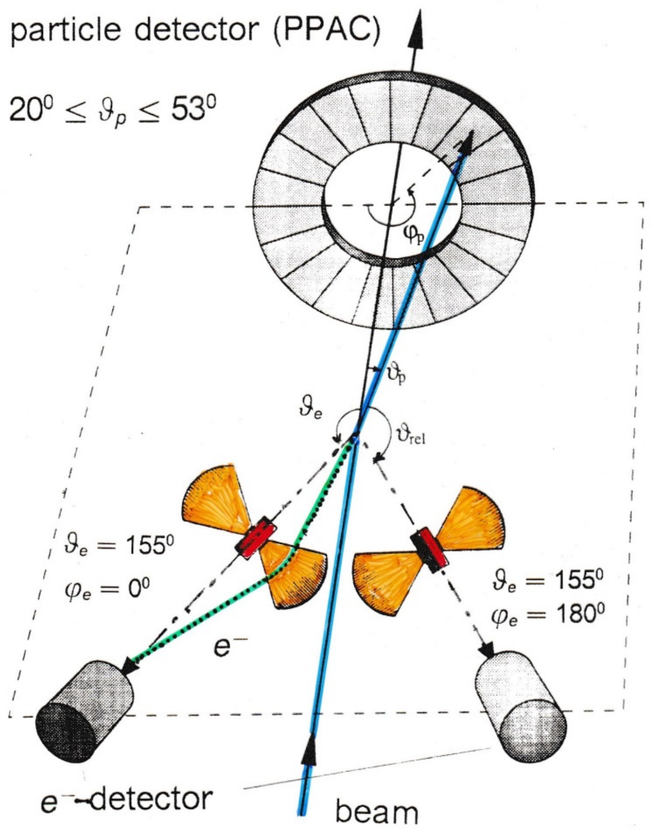

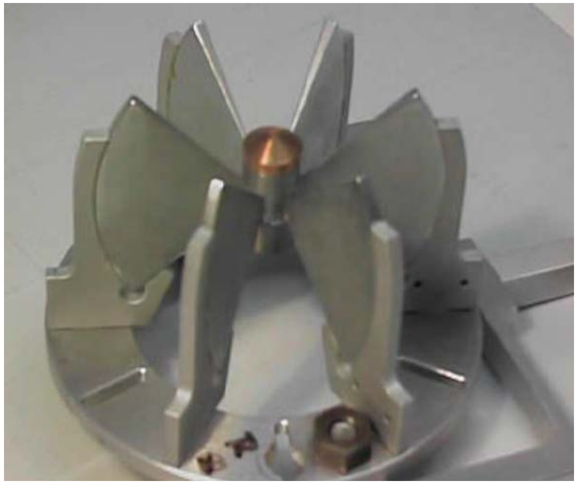

$\Delta\vartheta_e = 20^0$
target – Mini-Orange: 19 cm
Mini-Orange – Si detector: 6 cm

Doppler correction for projectile excitation:

$$\boxed{T_e^* = \gamma \cdot T_e \cdot \left\{1 - \beta_1 \cdot \sqrt{1 + 2m_e\, c^2/T_e} \cdot cos\theta_{e1}\right\} + m_e c^2 \cdot (\gamma - 1)}$$

$$cos\theta_{e1} = cos\vartheta_1 cos\vartheta_e + sin\vartheta_1 sin\vartheta_e cos(\varphi_e - \varphi_1)$$

Doppler-corrected e$^-$ and γ-ray spectrum

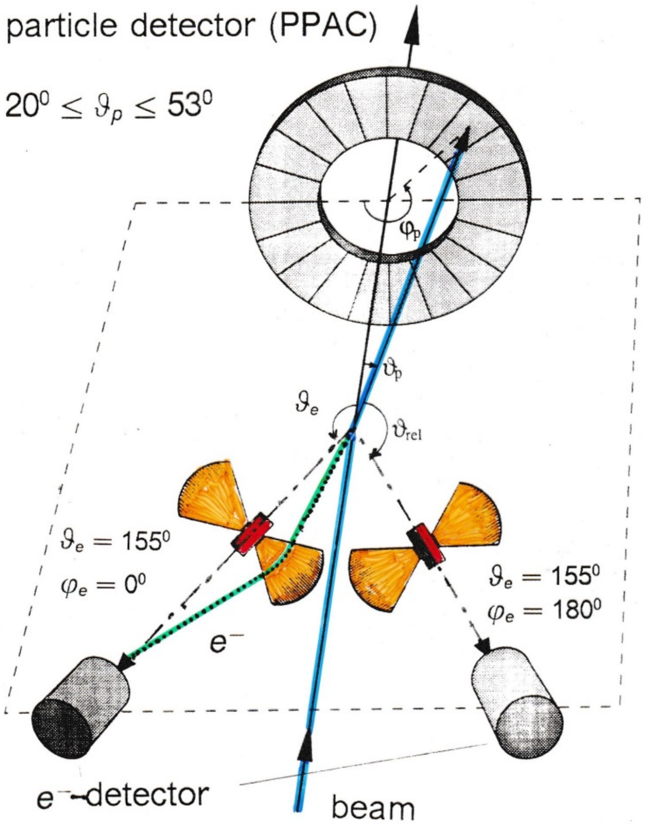

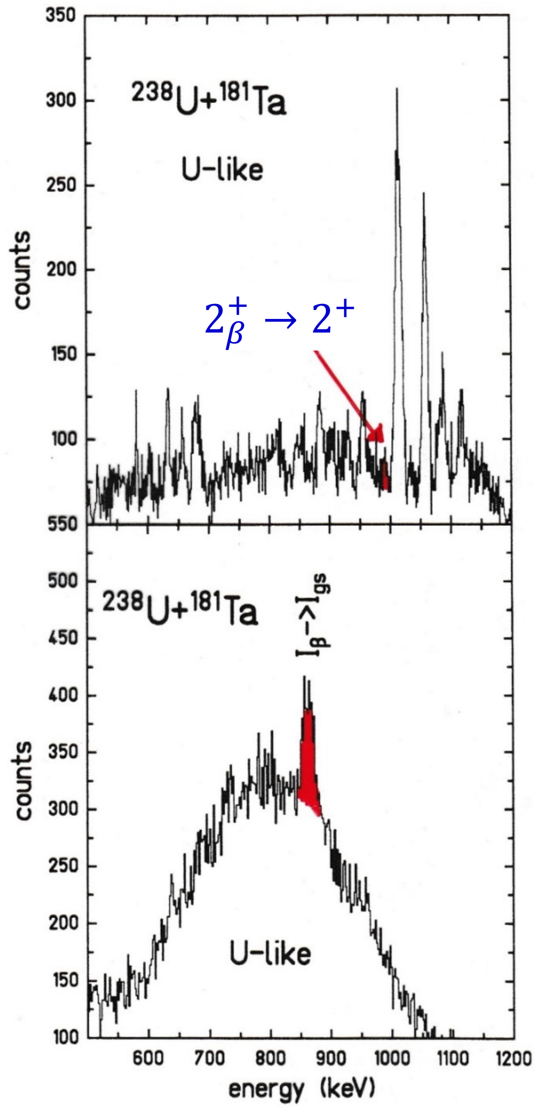

γ-ray spectrum

e$^-$ spectrum

Electron spectroscopy

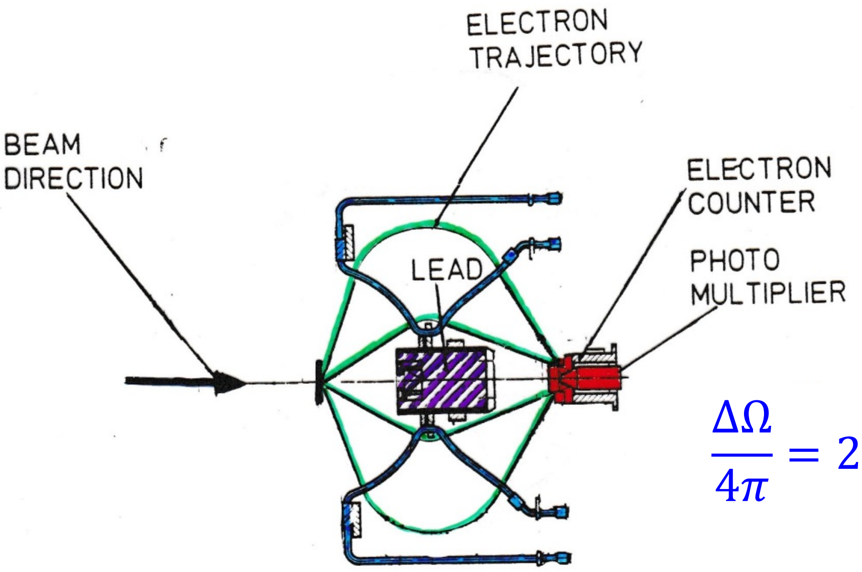

$$\frac{\Delta\Omega}{4\pi} = 26\%$$

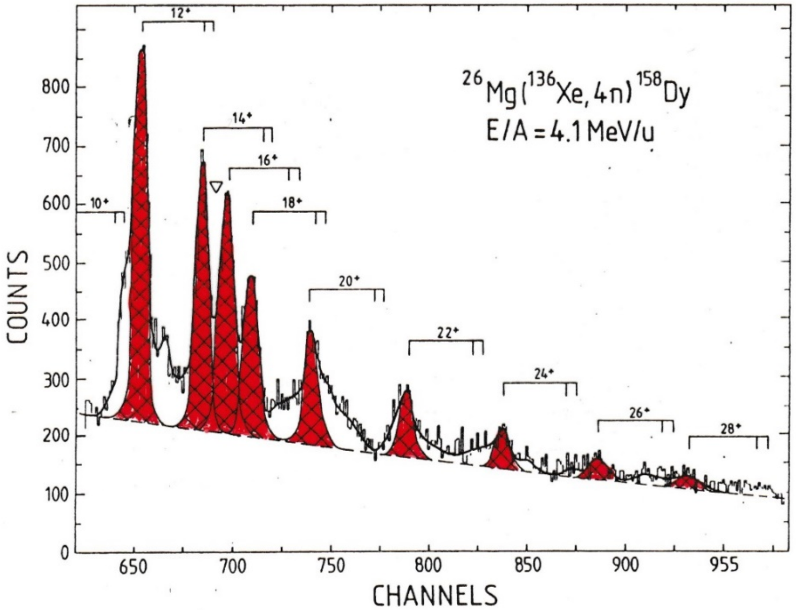

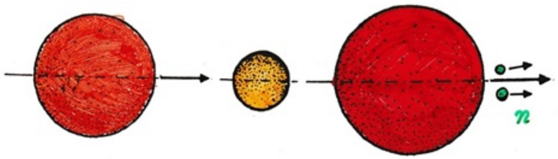

$^{136}Xe + ^{26}Mg \rightarrow ^{158}Dy$

$\vartheta_c = 0^0$

$\beta_c = \beta_{cm} = 0.079$

		$(\frac{\Delta p}{p})_e / \%$
resolution of the spectrometer including Doppler correction as calculated for a point source		0.4
scattering in the target	(i)	0.004
beam optics	(ii)	0.11
evaporation of neutrons	(iii)	0.09
energy loss in the target	(iv)	0.31
energy straggling of the projectiles	(v)	0.006
quadratic sum		0.53
experimental resolution		0.56

%

L. Handschug et al.; NIM 161 (1979) 117

Nuclear structure of ^{178}Hf

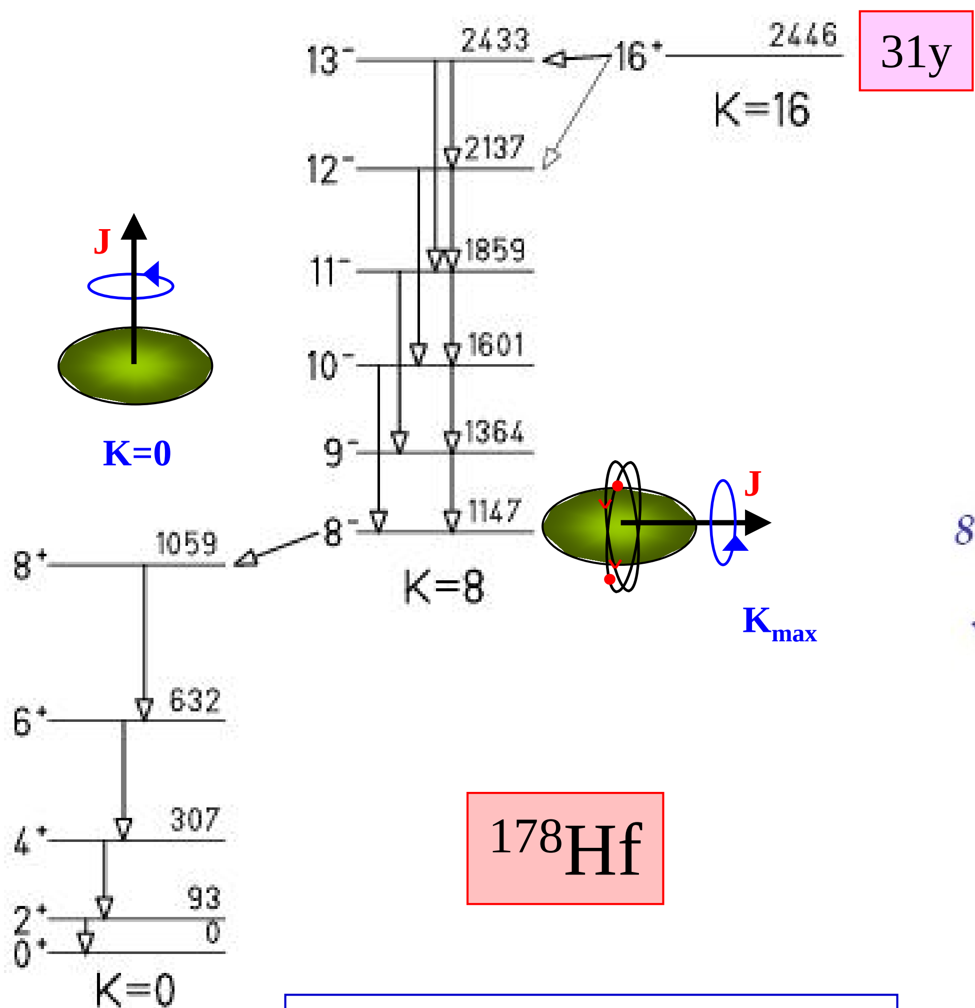

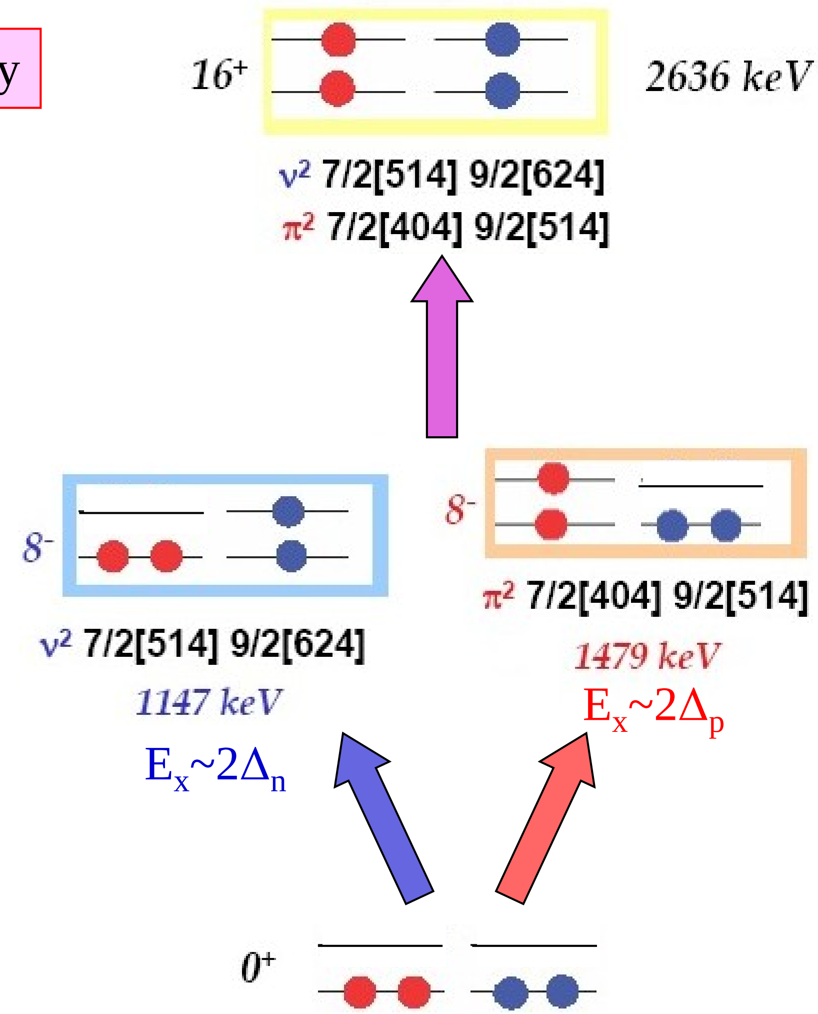

high-K orbitals near the Fermi surface

$\nu: f_{7/2}\, i_{13/2} \quad \pi: h_{11/2}\, g_{7/2}$

Coulomb excitation of the K = 8 isomer in ^{178}Hf

- ^{178}Hf + ^{130}Te at 560, 590, 620 MeV

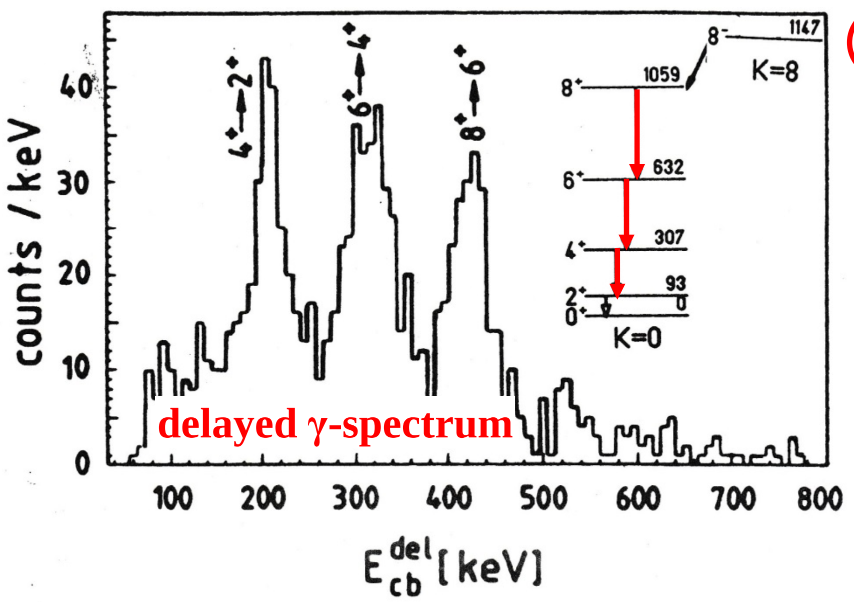

4 s $\rightarrow M_{30}\ (E3)$

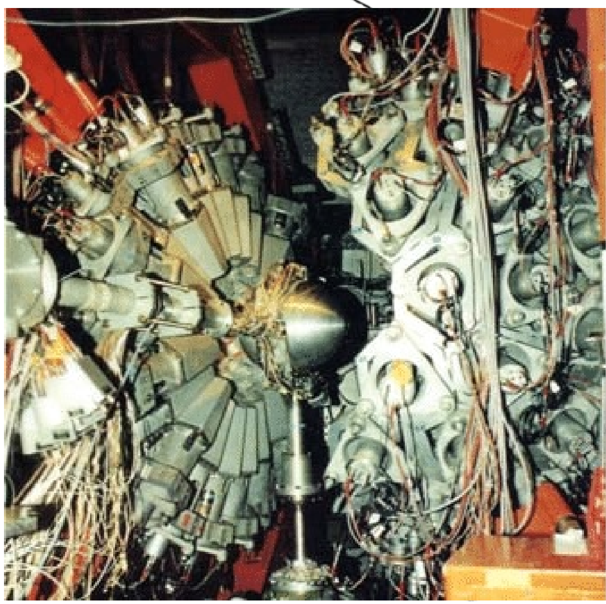

Delayed γ-ray spectrum of the Crystal Ball with $850 keV \leq E_{sum}^{del} \leq 1100 keV$ and $3 \leq N_{det} \leq 6$. In addition at least one of the delayed γ-rays must have been detected in one of the Ge-detectors.

Darmstadt Heidelberg Crystal Ball

ΔE_{γ} = 90 keV

Transient magnetic fields

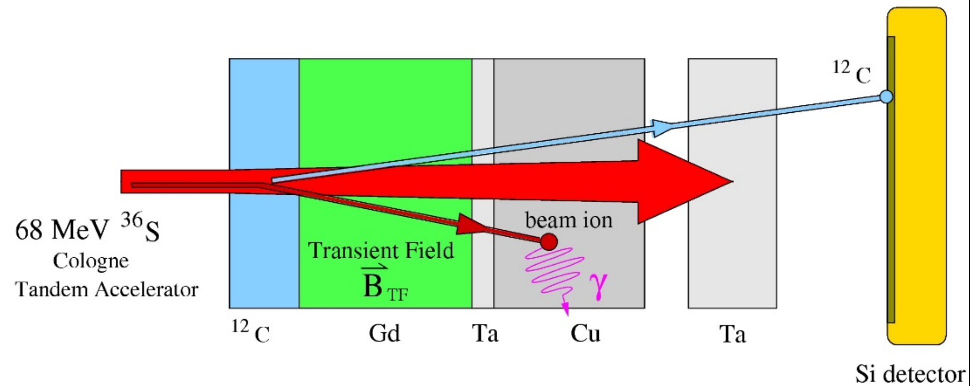

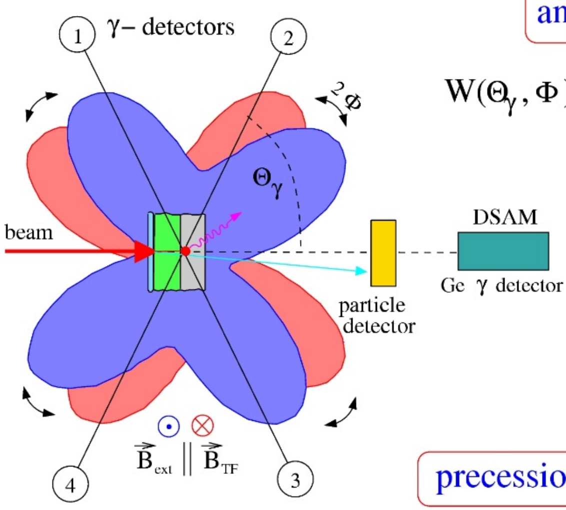

angular correlation

$$W(\Theta_\gamma, \Phi) = \sum_{k=0,2,4,..}^{k_{max}} Q_k \cdot A_k \cdot P_k\,(\cos(\Theta_\gamma \pm \Phi))$$

double ratio:

$$DR(1/4) = \frac{N1\uparrow}{N1\downarrow} \div \frac{N4\uparrow}{N4\downarrow}$$

precession angle

$$\Phi = \frac{\sqrt{DR} - 1}{\sqrt{DR} + 1} \Big/ \frac{1}{W} \cdot \left.\frac{dW}{d\Theta}\right|_{\Theta_\gamma} = g\,\frac{\mu_N}{\hbar} \int_{t_{in}}^{t_{out}} B_{TF}(v_{ion})\, e^{-\frac{t}{\tau}}\, dt$$

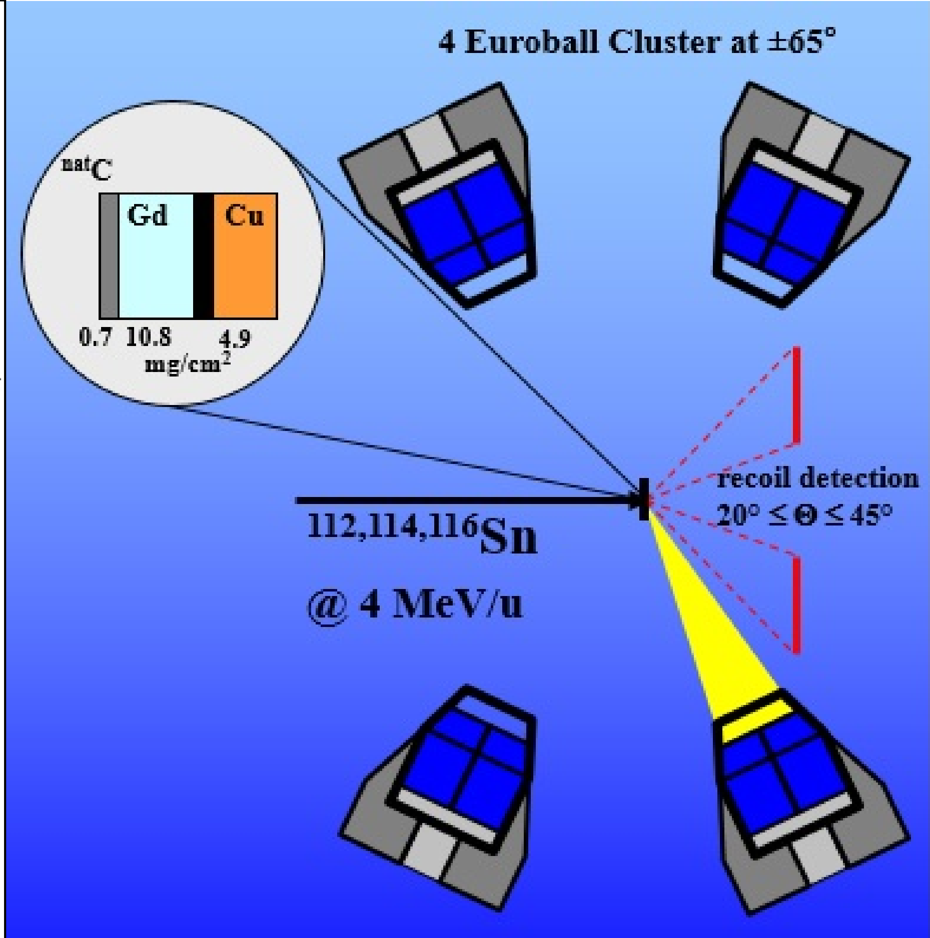

Spectroscopy of binary and ternary fission fragments

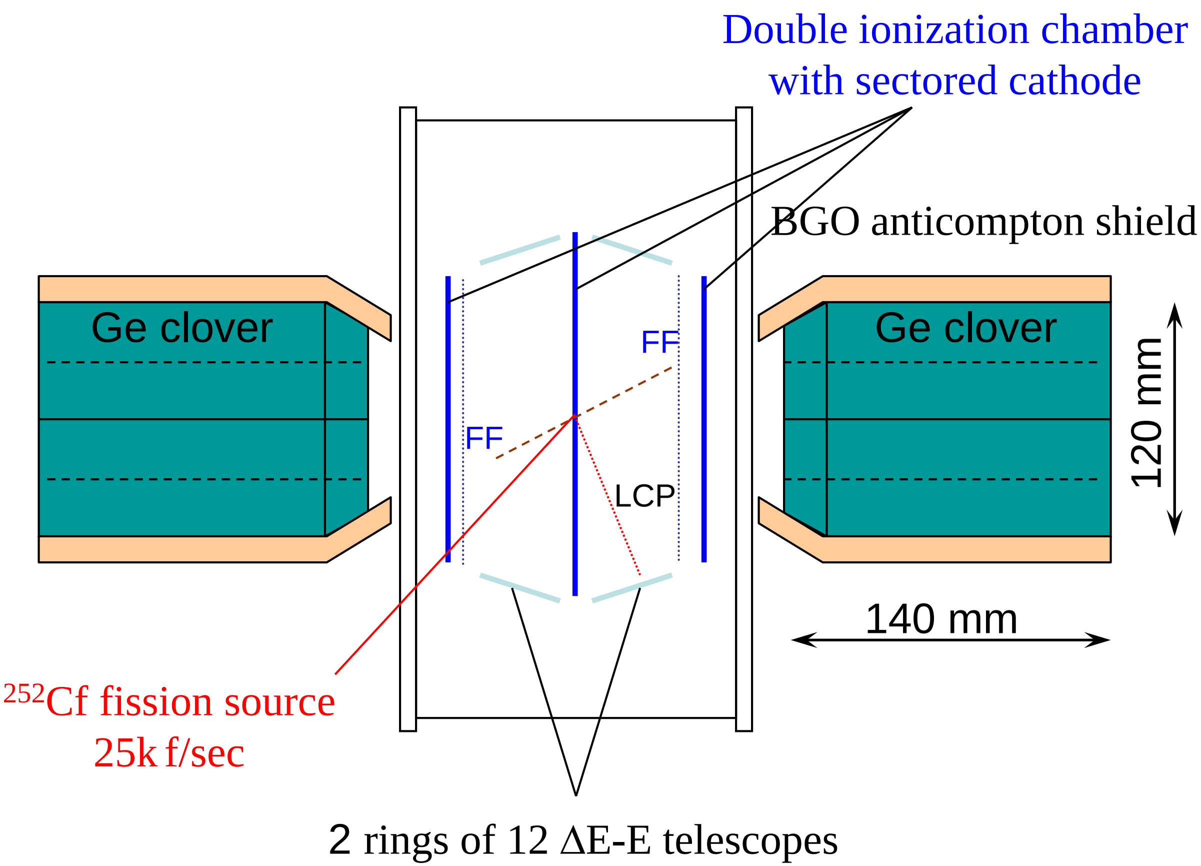

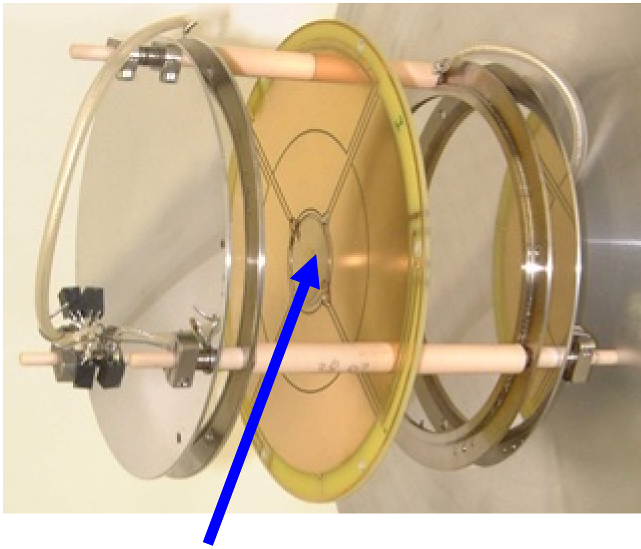

^{252}Cf source (25k f/s)

$T_{1/2}$=2.645y

E_α = 6.118 and 6.076 MeV

bin. fiss./α-decay = 1/31

ter. fiss./α-decay = 1/8308

4π twin ionization chamber for fission fragments

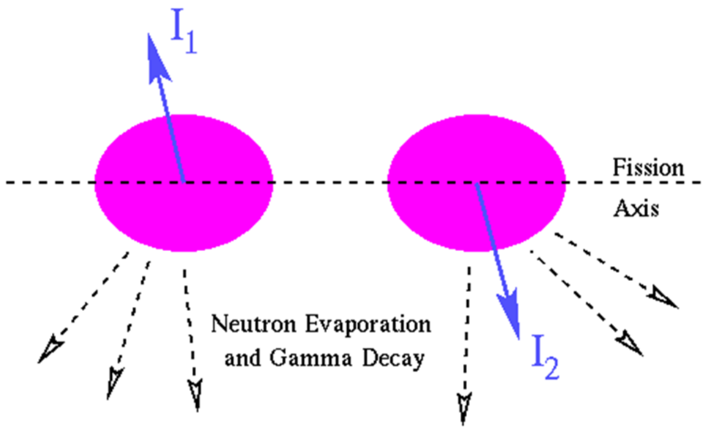

The origin of fragment spins and their alignment

$4^+ \rightarrow 2^+$ transitions

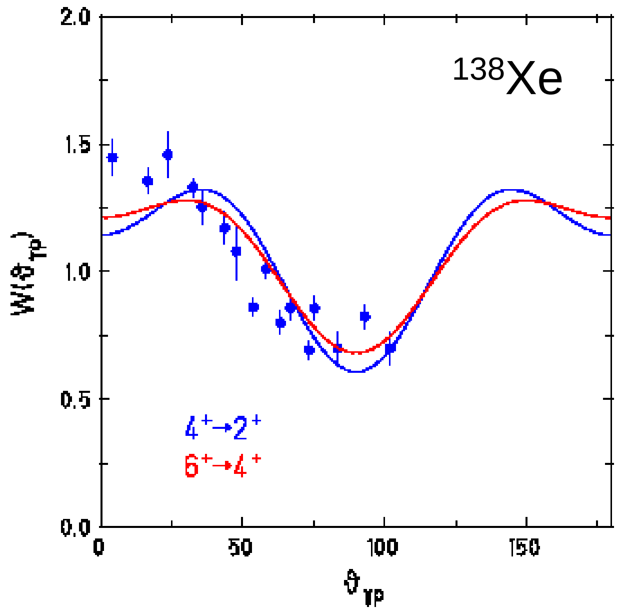

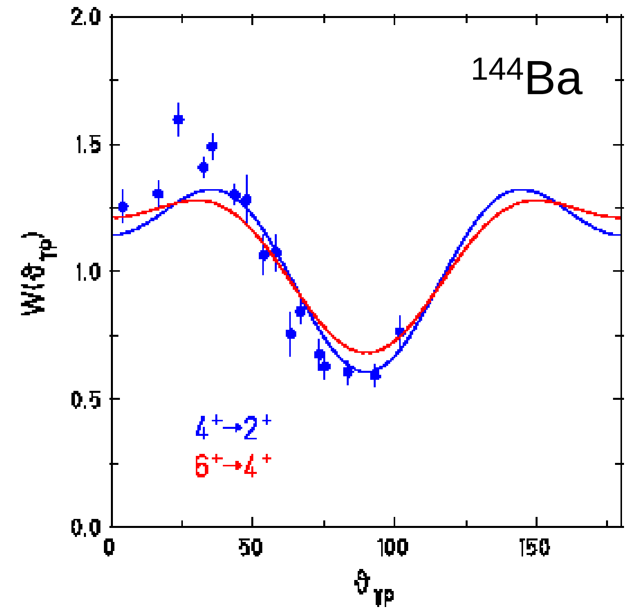

Open problems

- Coulomb excitation of isomeric states in deformed nuclei
- Nuclear structure of ^{208}Pb
- Studies in the ^{100}Sn region (Magda Gorska)
- Search for diabolic pair transfer at higher angular momentum states

- Mini Orange devices from Johan van Klinken are with Torsten Kröll (TU Darmstadt)

- 10 radioactive targets (0.3 mg/cm^2) from LMU München stored in Mainz (C. Düllmann)
  ^{235}U (1 mg ≡ 80 Bq), ^{237}Np (1 mg ≡ 26 kBq), ^{242}Pu (1 mg ≡ 145 kBq) (area = 0.2 cm^2)
  ^{226}Ra material